

# Synthesis and Characterization of New Heterometallic Cobalt-zinc Oxalates Linked by Organic Amines

ILDIKO BUTA<sup>1</sup>, CATALIN IANASI<sup>1</sup>, CECILIA SAVII<sup>1\*</sup>, LILIANA CSEH<sup>1</sup>, SNEJANA BAKARDIEVA<sup>2</sup>, WOLFGANG LINERT<sup>3</sup>, OTILIA COSTISOR<sup>1\*</sup>

<sup>1</sup>Institute of Chemistry Timisoara of Romanian Academy, 24 Mihai Viteazu Bv, 300223 Timisoara, Romania

<sup>2</sup>Institute of Inorganic Chemistry of the ASCR, v.v.i., Husinec-Rež 1001, 250 68 Rež, Czech Republic

<sup>3</sup>Institute of Applied Synthetic Chemistry, Vienna University of Technology, Getreidemarkt, 9/163-AC, 1060 Vienna, Austria

*Our research interest was related to the synthesis of polynuclear metal complexes containing oxalate as ligand with the aim of obtaining potentially new functional materials and precursors for oxide nanoparticles. Two new heteronuclear complexes  $\text{Co}_2\text{Zn}_2(\text{C}_{10}\text{H}_8\text{N}_2)_3(\text{C}_2\text{O}_4)_4 \cdot 2\text{H}_2\text{O}$ , 1, and  $\text{CoZn}(\text{C}_4\text{H}_{10}\text{N}_2)(\text{C}_2\text{O}_4)_2 \cdot 0.75\text{H}_2\text{O}$ , 2, were obtained by direct metal-ligand synthesis. Based on UV-Vis, IR, Raman and elemental analysis, a polymeric tridimensional structure of complexes was established, in which metal-oxalate chains are bridged by 4,4'-dipyridine or piperazine. Morphological characters have been proved by BET and SEM measurements. Scanning electron microscopy shows particles as assemble of parallel porous sheets for complex 1 and rods and hollow rod-like particles for complex 2. The surface area and porosity were evaluated from the nitrogen adsorption-desorption isotherms. Complex 1 presents mesoporous morphology with the surface area of  $29.9 \text{ m}^2/\text{g}$  while complex 2 was also porous, with the surface area of  $84.3 \text{ m}^2/\text{g}$  due to the more complex morphology. Thermo-gravimetric analysis showed that the decomposition proceeds via three well-defined steps up to final residue expressed as cobalt and zinc oxides for both complexes.*

**Keywords:** polynuclear ZnCo complexes; oxalate; organic co-ligands; functional materials mesoporous morphology; hollow rod-like particles

The versatility of the oxalate ligand leads to a great variety of metal complexes which attracted interest mainly on their morphological aspects and the resulting properties. Among them, homo- and heterometallic [1, 2], coordination polymers of ribbon infinite chain [3-5], 2D [6, 7] and 3D [8] structures have been obtained in which oxalate acting as bis-bidentate ligand bridges two or more metal ions. The strong magnetic interaction mediated by oxalate ligand has been used in search for new molecular – based magnetic materials [9, 10]. In order to obtain a controlled structure, organic co-ligands, including di- or polyamines like 4,4'-dipyridine and piperazine has been used as directing ligands and spacers. It was found that piperazine [11], adopting a low energy conformation, coordinates two metal centers belonging to two metal oxalate chains. Additionally to this linkage, 4,4'-dipyridine is capable to develop  $\pi$ - $\pi$  stacked interactions leading to supramolecular architectures with specific crystallinity [12].

Monometallic oxalate forms of nanoribbons [13] or nanorods [14] were obtained by the reverse micellar route and used as new battery materials.

It was found that polymetallic oxalates can act as single source precursor, for the synthesis of various oxides in which the morphology of the precursors is preserved [15-20], phenomenon known as coordination memory. The preservation tendency of morphology is more pronounced for the oxalates than other metal carboxylates. Beside, oxalates easily decompose to their corresponding oxides [21]. These properties can explain the expanded trends of use of oxalates as precursors for a wide variety of mixed metal oxides nanoparticles with designed properties and industrial importance [10]. The recent literature research revealed the focused interest on the zinc-cobalt spinels

with relevance in many industrial applications such as pigments or dyeing materials, as catalysts [22], as anode material in lithium batteries [23] and in supercapacitor applications [24]. For example, the obtaining of the precursor  $\text{ZnCo}_2(\text{C}_2\text{O}_4)_3 \cdot 6\text{H}_2\text{O}$  was reported as nanoparticles by a one-step solid state reaction [25]. Changchun and all [24] reported the obtaining of  $\text{ZnCo}_2\text{O}_4$  spinel by calcination of a mixed metal oxalate obtained by rheological phase reaction. However, in both of cases the nature of the bimetallic oxalates as precursors was not proved by any physical or chemical methods. In previous studies we reported heteronuclear metal oxalates [26] and, for some of them, catalytic properties were demonstrated.

Our present research interest is related to the synthesis of polynuclear metal complexes containing oxalate as ligand in order to obtain new functional materials and precursors for oxide nanoparticles. We report here the synthesis and primary characterization of new heterometallic oxalates in the cobalt(II) – zinc(II) system containing 1,10-dipyridyl or piperazine as co-ligands having in mind that they can act as catalysts or precursors for bimetallic oxides.

## Experimental part

All chemicals used for the present study were purchased from commercial sources and used without further purification.

Elemental analyses were carried out on a Perkin-Elmer model 240C elemental analyzer. The infrared (IR) spectra of samples were recorded on a Jasco FT/IR-430 spectrometer in the range  $4000\text{--}400 \text{ cm}^{-1}$  on KBr pellets. FT-Raman spectra were recorded on a Jasco Raman NRS 3300 spectrometer, with excitation wavelength of 785 nm, spectral resolution of  $0.65 \text{ cm}^{-1}$ . Electronic absorption

\* email: ocostisor@acad-icht.tm.edu.ro; ceciliasavii@yahoo.com;  
Tel.: +40-256-491818

spectra were recorded in nujol on a Lambda 12 Perkin-Elmer spectrophotometer. Thermal analysis was carried out under static air at a heating rate of 10 K/min from 20 to 900°C using a Netzsch STA 409 PC/PG instrument. The morphology of the samples was examined with scanning electron microscopy, SEM PHILIPS XL 30 CP, coupled with detectors: SE, BSE, Robinson and EDX. Opp', N<sub>2</sub> adsorption-desorption isotherms of the samples were recorded on a Quantachrome Nova 1200e, at 77 K. The samples were degassed at room temperature for 3 h under vacuum, prior to the adsorption measurements.

*Co<sub>2</sub>Zn<sub>2</sub>(C<sub>10</sub>H<sub>8</sub>N<sub>2</sub>)<sub>3</sub>(C<sub>2</sub>O<sub>4</sub>)<sub>4</sub> · 2H<sub>2</sub>O (1)* 0.5 g (2 mmol) Co(CH<sub>3</sub>COO)<sub>2</sub> · 4H<sub>2</sub>O dissolved in 10 ml water was treated with 0.64 g (4 mmol) 4,4'-dipyridine, 0.3 g (2 mmol) ZnCl<sub>2</sub> and 0.6 g (4 mmol) (NH<sub>4</sub>)<sub>2</sub>C<sub>2</sub>O<sub>4</sub> · H<sub>2</sub>O under stirring. The mixture was heated at 80°C for one hour. The pink solid was collected by filtration, washed with diluted ammonium oxalate solution, water and ethylic alcohol and dried over CaCl<sub>2</sub>.

Anal. Calc. for C<sub>38</sub>H<sub>28</sub>N<sub>6</sub>Co<sub>2</sub>Zn<sub>2</sub>O<sub>18</sub> (M = 1105.30) %: C 41.29; H 2.55; N 7.60; Co 10.66; Zn 11.83. Found %: C 41.09; H 2.41; N 7.17; Co 10.62; Zn 11.41;

IR (KBr, ν/cm<sup>-1</sup>): 3373m, 3053w, 2923w, 1602s, 1408m, 1358w, 1312m, 1220w, 1076w, 1001w, 855w, 807m, 739w, 623m, 577w, 502m.

Raman: 1608s, 1515m, 1460m, 1448sh, 1427w, 1299s, 1238m, 1229sh, 1084m, 1016s, 997m, 903w, 878w, 863w, 767m, 672w, 655m, 574m, 533w, 506m, 391m, 337m, 292w, 273w, 241w, 214m, 108m.

UV - VIS (nujol): λ = 550 nm, 630 nm.

*CoZn(C<sub>10</sub>H<sub>8</sub>N<sub>2</sub>)(C<sub>2</sub>O<sub>4</sub>)<sub>2</sub> · 0.75H<sub>2</sub>O (2)* 0.5 g (2 mmol) Co(CH<sub>3</sub>COO)<sub>2</sub> · 4H<sub>2</sub>O dissolved in 10 mL water, was treated with 0.78 g (4 mmol) piperazine, 0.3 g (2 mmol) ZnCl<sub>2</sub> and 0.6 g (4 mmol) (NH<sub>4</sub>)<sub>2</sub>C<sub>2</sub>O<sub>4</sub> · H<sub>2</sub>O under constant stirring. The mixture was heated at 80°C for one hour. The pink solid was collected by filtration, washed with diluted ammonium oxalate solution, water and ethylic alcohol, and dried over CaCl<sub>2</sub>.

Anal. Calc. for C<sub>18</sub>H<sub>11.5</sub>N<sub>2</sub>CoZnO<sub>8.75</sub> (M = 400.00) %: C 24.02; H 2.90; N 7.00; Co 14.73; Zn 16.35; Found %: C 23.62; H 2.69; N 7.12; Co 14.77; Zn 16.52.

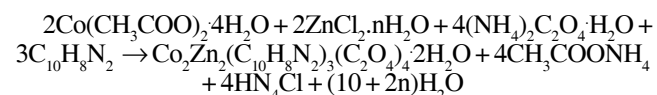
IR (KBr, ν/cm<sup>-1</sup>): 3373s, 2133w, 1628s, 1358m, 1317m, 1234m, 819m, 754m, 608m, 495m, 466w.

Raman: 1617w, 1460s, 1430sh, 910m, 855w, 584m, 529s, 450w, 240s, 219m, 199m, 126m.

UV - VIS (nujol): λ = 560 nm, 680 nm.

## Results and discussions

The new heteronuclear complexes Co<sub>2</sub>Zn<sub>2</sub>(C<sub>10</sub>H<sub>8</sub>N<sub>2</sub>)<sub>3</sub>(C<sub>2</sub>O<sub>4</sub>)<sub>4</sub> · 2H<sub>2</sub>O (1) and CoZn(C<sub>10</sub>H<sub>8</sub>N<sub>2</sub>)(C<sub>2</sub>O<sub>4</sub>)<sub>2</sub> · 0.75H<sub>2</sub>O (2) have been obtained by direct metal-ligand synthesis as pink microcrystalline powders in aqueous media. Typical methods are presented in the experimental part and the synthesis of 1 is shown in scheme 1:



Scheme 1. Synthesis chemical reaction of complex 1

The compounds are insoluble in water and in common polar organic solvents like alcohols, acetone, acetonitrile, dimethylformamide and dimethylsulphoxide. The nature of the resulted compounds was established based on

elemental analysis and structural information was obtained from electronic, FT-IR and FT-Raman spectra.

## Electronic spectra

The electronic spectra of the two complexes show the presence of two ligand-field transitions: one near 550 nm and the second at 630 and 680 nm, respectively. According to Lever [27], the bands can be assigned to the (v<sub>3</sub>) <sup>4</sup>T<sub>1g</sub>(P) ← <sup>4</sup>T<sub>1g</sub> and (v<sub>2</sub>) <sup>4</sup>A<sub>2g</sub> ← <sup>4</sup>T<sub>1g</sub> transition, respectively, characteristic to a high-spin d<sup>7</sup> ion in a distorted-octahedral environment.

## Infrared and Raman spectra

The infrared spectra of the new compounds are very complex. However, bands attributable to the oxalate and organic N-donor ligands can be noticed. In the spectra of the both complexes the asymmetric stretching mode ν<sub>3</sub>(OCO) emerged at 1602 cm<sup>-1</sup> for (1) and 1628 cm<sup>-1</sup> for (2). This mode is also Raman active as a strong band at 1608 cm<sup>-1</sup> for (1) and a weak one at 1617 cm<sup>-1</sup> for (2). The ν<sub>5</sub>(OCO) mode can be noticed as doublets at 1358, 1312 and 1358, 1317 cm<sup>-1</sup> for (1) and (2), respectively. For both complexes, Raman spectra show for this mode a medium intense band at 1460 with shoulders at 1448 for (1), and 1430 cm<sup>-1</sup> for (2). In the region 807 - 819 cm<sup>-1</sup> of the infrared spectra, bands attributable to the deformation vibration mode δ(OCO) can be noticed. According to Frost [28], in the Raman spectra, the low intensity bands at 878 cm<sup>-1</sup> (1) 854 cm<sup>-1</sup> (2) respectively are assigned to the δ(OCO) bending mode. The observed values agree well with those reported for the presence of bis-chelating oxalate ion [29].

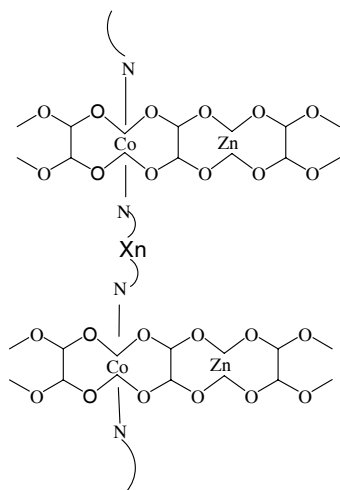
The presence of 4,4'-bipyridyl ligand in complex 1 is proved by the bands at 3053 cm<sup>-1</sup> assigned to ν(C<sub>sp</sub>-H), and 1408 cm<sup>-1</sup>, 1220 cm<sup>-1</sup> assigned to ν(C-C) and ν(C-N) valence vibrations of aromatic rings, respectively. The γ(C-H) out-of-plane vibrations can be noticed at 739 cm<sup>-1</sup>. Also the pyridine "breathing" frequency appearing at 993 and 612 cm<sup>-1</sup> in free ligand is shifted to 1001 and 623 cm<sup>-1</sup> respectively in the spectra of the complexes. In the Raman spectrum, the weak band at 997 cm<sup>-1</sup> is assigned to the γ(C-H) out-of-plane bending vibration, the band at 391 cm<sup>-1</sup> to the pyridil ring and γ(C-C) out-of-plane bending vibration [30].

In the IR spectrum of 2, the ν<sub>3</sub>(C-N) asymmetric stretching vibration at 1270 cm<sup>-1</sup> in the free piperazine is shifted to 1234 cm<sup>-1</sup>. The deformation vibration frequency of CCN moiety emerges at 608 cm<sup>-1</sup> and the valence vibration of M-N is present at 466 cm<sup>-1</sup>. Further, the absence of the band at 2800 cm<sup>-1</sup> characteristic to ν(N<sup>pip</sup>-CH<sub>2</sub>) in the spectrum of 2 denoting the presence of the coordinated piperazine in energetically stable *chair* conformation. According to [31] the bands at 910, 450 cm<sup>-1</sup> in the Raman spectrum of complex 2 can be assigned to the ν(C-N) stretching mode and δ(CCN) deformation vibration mode, respectively.

For both complexes, the presence of coordinated water is pointed out by the strong and large band at 3373 cm<sup>-1</sup>.

Based on above presented analytical data, spectral properties and literature, we propose a polymeric structure of complex 1 and 2. The metal ions cobalt (II) and zinc (II) are held together by the bis-bidentate oxalate bridge leading to chains that further are connected by 4,4'-dipyridyl or piperazine bridges bonded via nitrogen atoms. The proposed structure of complex 1 and 2 illustrating their polymeric nature is presented in scheme 2.

The overall arrangement can consist of interpenetration of two dimensional networks thus leading to a tridimensional structure. The crystal structure of the complexes is assumed to be stabilized by hydrogen



Scheme 2. Proposed structure for complex 1 ( $n=1$ , fragment from 4,4'-dipyridil) and 2 ( $n=2$ , fragment from piperazine)

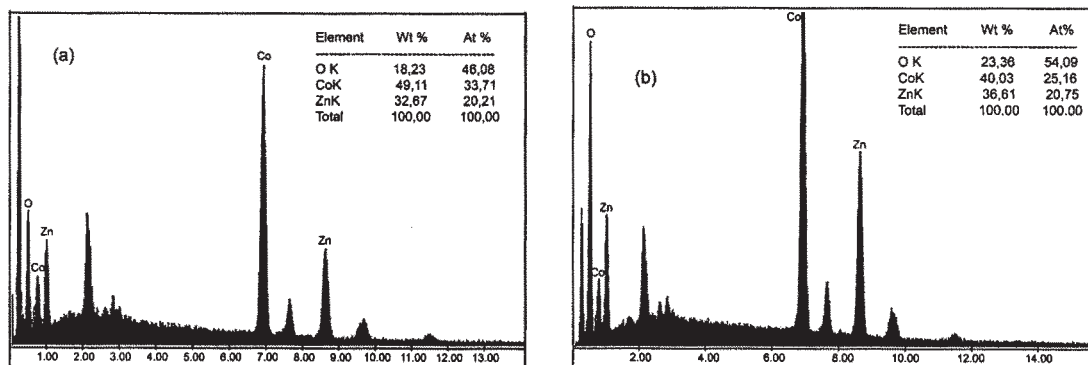


Fig. 1. EDX spectra of the complex (a) 1 and (b) 2

bindings which involve the water molecules and the oxygen atoms of the oxalate ligand. Moreover, for 1, the stabilization can be achieved by the  $\pi$ - $\pi$  stacking interactions between the pyridine rings.

#### EDX analysis

The EDX analysis of the samples showed the ratio between Co(II) and Zn(II) to be 1:1 (fig. 1) which is consistent with previous results.

#### SEM analysis

SEM studies of complex 1 and 2 were undertaken. The complex 1 figure 2 presents mica-like aggregates, forming particles as assemblies of parallel porous sheets.

The second one, complex 2 aggregates (fig. 3) as rod-like with wide aspect ratio and distribution, figure 4(a), and hollow rod-like, (fig. 4b), particles with relative homogenous dimensional distribution; rod's length is situated between tenths of nanometers to ~20 micrometers and diameter of ~1micrometre.

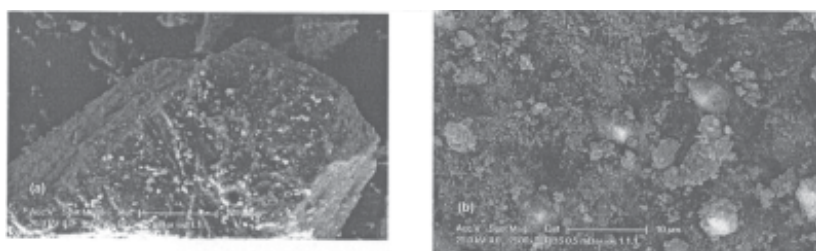


Fig. 2. SEM images of 1 at (a) x 250 and (b) x 2500 magnification

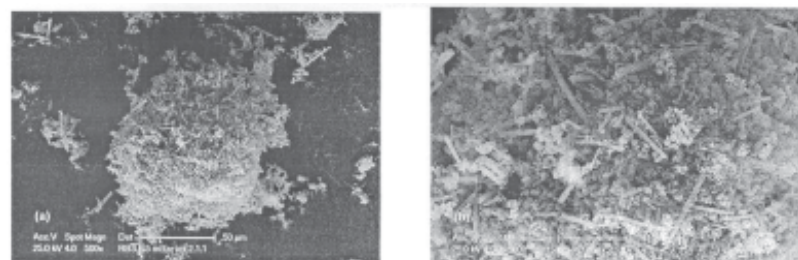


Fig. 3. SEM images of 2 at (a) x 500 and (b) x 1500 magnification

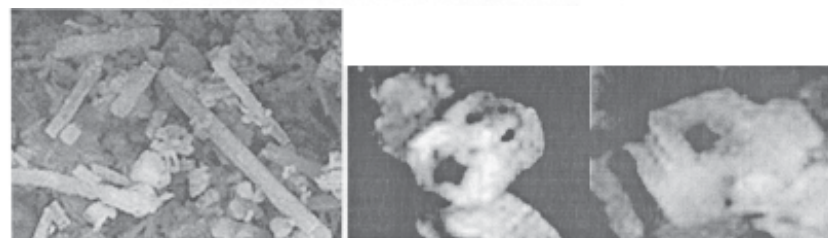


Fig. 4. SEM pictures (details) of rods (a) and cubic hollow (b) particles of 2



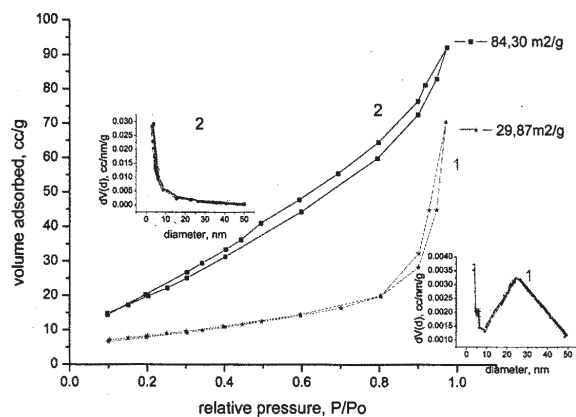


Fig. 5. Nitrogen adsorption-desorption isotherms:  
 $\text{Co}_2\text{Zn}_2(\text{C}_{10}\text{H}_8\text{N}_2)_3(\text{C}_2\text{O}_4)_4 \cdot 2\text{H}_2\text{O}$  (1) and  
 $\text{CoZn}(\text{C}_4\text{H}_{10}\text{N}_2)(\text{C}_2\text{O}_4)_2 \cdot 0.75\text{H}_2\text{O}$  (2)

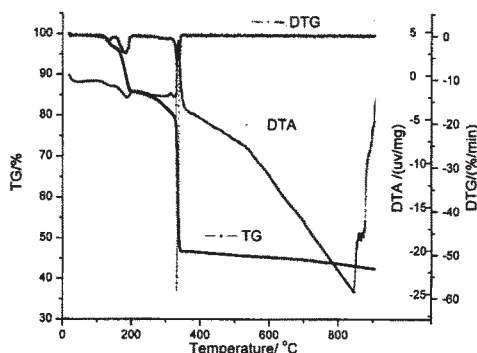
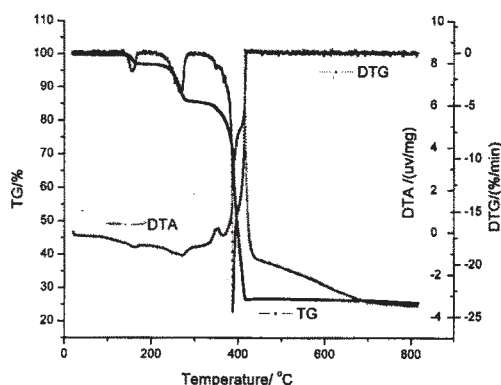


Fig. 6. Thermograms of 1 (a) and 2 (b) in static air

Hollow cubes of  $\sim 1$  micrometer, with hollow interior of almost square shape ( $\sim 320 \times 320$  nm), and wall thickness of  $\sim 300$  nm, it was observed as well.

#### BET Analysis

In accordance to IUPAC (International Union of Pure and Applied Chemistry) classifications, both isotherms, (fig. 5), show a type IV pattern. The hysteresis loop, which resulted from capillary condensation in the mesopores (2–50 nm) seems to be slightly different for the two compounds. In figure 5, the hysteresis loop of complex 1 resembles type H3 IUPAC classification, resulting from slit-shaped pores between parallel layers, with a non-uniform size [32, 33].

The type H4 hysteresis loop can be attributed as better resemblance in case of complex 2 and it is believed to be associated with narrow-slit pores of varying diameter; more likely the pore size distribution is shifted toward the micropore range.

Total BET surface area of complex 1 was  $29.87 \text{ m}^2/\text{g}$ . In the inset representation of pore diameters distribution, (fig. 5) it was observed a bimodal pore diameter distribution, around the values of 3.78 nm and 24.7 nm. The total BET surface area of complex 2 was  $84.30 \text{ m}^2/\text{g}$ . The complex 2 exhibited also a wide range of pore diameters figure 5 inset. It is possible that the difference between the morphology of the two compounds comes from the different template effect that the two co-ligands, 4,4'-bipyridine and piperazine, may have upon the metal oxalates.

The surface area observed for both complexes 1 and 2 of  $29.9 \text{ m}^2/\text{g}$  and  $84.3 \text{ m}^2/\text{g}$  is greater than the value found in literature for crystalline compounds with large grain size but highly agglomerated.

#### Thermal analysis

The thermal stability of compounds 1 and 2 correlated with their thermolysis products was determined by thermogravimetric and thermo-differential analysis (TG-DTA) in static air (fig. 6). It indicates that the decomposition of 1 and 2, in the range of temperature 0–800°C, proceeds

in three steps. The first weight loss, in both cases, associated with endothermic effect from 150 to 180°C for 1 and between 120 and 150°C for 2 was due to the loss of free water molecules [34–36]. The second weight loss was observed from 240 to 295°C for 1 and between 160 and 190°C for 2. This second step, also had an endothermic effect, it corresponds to complex phenomena that means the superposition of different thermal effects. It could be attributed to the decomposition of oxalate and the cleavage of N-Co bonds. Although, the oxalate oxidation is generally an exothermic process [36], the endothermic process of N-M bond cleavage has a greater enthalpy value, turning the overall process into an endothermic one.

The third weight loss ( $73.23\%$  for 1 and  $52.98\%$  for 2), from 320 to 425°C for 1 and respectively 240 to 350°C for 2, is due to the decomposition of organic phase (bipyridine and piperazine) and the formation of the following possible oxides: either  $\text{Co}_3\text{O}_4$  and  $\text{ZnO}$  or  $\text{ZnCo}$  spinels ( $\text{Zn}_{1/3}\text{Co}_{2/3}\text{O}_4$ ,  $\text{ZnCo}_2\text{O}_4$ ,  $\text{Co}_3\text{O}_4$  and  $\text{ZnO}$  [35, 37].

#### Conclusions

In summary, new heteronuclear complexes  $\text{Co}_2\text{Zn}_2(\text{C}_{10}\text{H}_8\text{N}_2)_3(\text{C}_2\text{O}_4)_4 \cdot 2\text{H}_2\text{O}$  (1) and  $\text{CoZn}(\text{C}_4\text{H}_{10}\text{N}_2)(\text{C}_2\text{O}_4)_2 \cdot 0.75\text{H}_2\text{O}$  (2) were obtained by direct metal–ligand reaction. IR and Raman spectra are in agreement, both show the presence of the bis-bidentate bridging form of the oxalate and the coordinated ligands. From electronic spectra was established distorted-octahedral configuration for Co(II) in both compounds and elemental analysis proves the presence of the two metal ions in molar ratio 1:1. The metal/metal ratio was confirmed also by EDX analysis on solid compounds. SEM and BET measurements sustain the proposed structure and morphology of heteronuclear complexes. Complex 1 is composed by particles as assemblies of parallel porous sheets that could be formed from flat primary crystallites. Complex 2 aggregate as rod-like particles with wide aspect ratio and distribution, and hollow cube-like particles with relative homogenous dimensional distribution.

### Acknowledgements

*The authors acknowledge the supports of the Romanian Academy, Bilateral cooperation program Institute of Chemistry Timisoara of Romanian Academy - Technical University Vienna, Austria and Interacademic exchange program Romania - Czech Republic. The authors cordially thank Mr. Mike Tucker of Quantachrome Corporation for useful comments and insightful discussions.*

### Reference

1. CORONADO E., GALÁN-MASCARÓS J.R., GIMÉNEZ-SAIZ C., GÓMEZ-GARCÍA C.J., RUIZ PÉREZ C., TRIKI S., *Adv. Mater.*, **8**, no. 9, 1996, p. 737
2. ALBEROLA A., CORONADO E., GIMÉNEZ-SAIZ C., GÓMEZ-GARCÍA C.J., ROMERO F.M., TARAZÓN A., *Eur. J. Inorg. Chem.*, **2**, 2005, p. 389
3. CASTILLO O., LUQUE A., JULVE M., LLORET F., ROMÁN P., *Inorg. Chim. Acta.*, **315**, no. 1, 2001, p. 9
4. CASTILLO O., LUQUE A., ROMÁN P., LLORET F., JULVE M., *Inorg. Chem.*, **40**, no. 22, 2001, p. 5526
5. WU W.Y., SONG Y., LI Y.Z., YOU X.Z., *Inorg. Chem. Commun.*, **8**, no. 8, 2005, p. 732
6. CORONADO E., GALÁN-MASCARÓS J.R., GÓMEZ-GARCÍA C.J., MARTÍNEZ-FERRERO E., ALMEIDA M., WAERENBORGH J. C., *Eur. J. Inorg. Chem.*, **11**, 2005, p. 2064
7. TAMAKI H., MITSUMI M., NAKAMURA K., MATSUMOTO N., KIDA S., OKAWA H., IJIMA S., *Chem. Lett.*, 1992, p. 1975
8. DECURTINS S., SCHMALLE H.W., PELLAUX R., HUBER R., FISCHER P., OULADDIAF B., *Adv. Mater.*, **8**, no. 8, 1996, p. 647
9. PELLAUX R., SCHMALLE H.W., HUBER R., FISCHER P., HAUSS T., OULADDIAF B., DECURTINS S., *Inorg. Chem.*, **36**, no. 11, 1997, p. 2301
10. CORONADO E., GALÁN-MASCARÓS J.R., *J. Mater. Chem.*, **15**, no. 1, 2005, p. 66
11. KEENE T.D., HURSTHOUSE M.B., PRICE D.J., *Z. Anorg. Allg. Chem.*, **630**, no. 3, 2004, p. 350
12. JANIÁK C., *J. Chem. Soc. Dalton Trans.*, **21**, 2000, p. 3885
13. ARAGÓN M.J., LEÓN B., PÉREZ-VICENTE C., TIRADO J.L., CHADWICK A.V., BARKO A., BEH S. Y., *Chem. Mater.*, **21**, no. 9, 2009, p. 1834
14. ARAGÓN M.J., LEÓN B., PÉREZ-VICENTE C., TIRADO J.L., *Inorg. Chem.*, **47**, no.22, 2008, p. 10366
15. ANGERMANN A., TÖPFER J., *J. Mat. Sci.*, **43**, no. 15, 2008, p. 5123
16. GABAL M.A., AHMED M.A., *J. Mat. Sci.*, **40**, no. 2, 2005, p. 387
17. GANGULY A., KUNDU R., RAMANUJACHARY K.V., LOFLAND S.E., DAS D., VASANTHACHARYA N.Y., AHMAD T., GANGULI A.K., *J. Chem. Sci.*, **120**, no. 6, 2008, p. 521
18. AHMAD T., CHOPRA R., RAMANUJACHARY K.V., LOFLAND S.E., GANGULI A.K., *J. Nanosci. Nanotech.*, **5**, no.11, 2005, p. 1840
19. BATTEN S.R., ROBSON R., *Angew. Chem. Int. Ed.*, **37**, no. 11, 1998, p. 1460
20. WANG Q., WU X., ZHANG W., SHENG T., LIN P., LI J., *Inorg. Chem.*, **38**, no. 9, 1999, p. 2223
21. CORONADO E., MARTÍ-GASTALDO C., GALÁN-MASCARÓS J.R., CAVALLINI M., *J. Am. Chem. Soc.*, **132**, no. 15, 2010, p. 5456
22. OMATA K., TAKADA T., KASAHARA S., YAMADA M., *Appl. Catal. A*, **146**, no. 2, 1996, p. 255
23. AI C., YIN M., WANG C., SUN J., *J. Mater. Sci.*, **39**, no. 3, 2004, p. 1077
24. KALPANA D., OMKUMAR K.S., KUMAR S.S., RENGANATHAN N.G., *Electrochem. Acta.*, **52**, no. 3, 2006, p. 1309
25. SONG F., HUANG L., CHEN D., TANG W., *Mat. Lett.*, **62**, no. 3, 2008, p. 543
26. COSTISOR O., BREZEANU M., JOURNAUX Y., MEREITER K., WEINBERGER P., LINERT W., *Eur. J. Inorg. Chem.*, **8**, 2001, p. 2061
27. LEVER ABP, *Inorganic Electronic Spectroscopy*, Elsevier Publishing Company, Amsterdam, 1968, p. 320
28. FROST R.L., *Anal. Chim. Acta.*, **517**, no. 1-2, 2004, p. 207
29. EDWARDS H.G.M., HARDMAN P.H., *J. Mol. Struct.*, **273**, 1992, p. 73
30. ZHUANG Z., CHENGA J., WANG X., ZHAO B., HANA X., LUOB Y., *Spectrochim. Acta. A*, **67**, no. 2, 2007, p. 509
31. GUNASEKARAN S., ANITA B., *Indian J. Pure & Appl. Phys. (IJPAP)*, **46**, no. 12, 2008, p. 833
32. LIAN P., ZHU X., LIANG S., LI Z., YANG W., WANG H., *Electrochim. Acta.*, **55**, no. 12, 2010, p. 3909
33. RIES A., SIMOES A.Z., CILENSE M., ZAGHETE M.A., VARELA J.A., *Mater. Charact.*, **50**, no. 2-3, 2003, p. 217
34. SUN Y. Q., ZHANG J., YANG G.Y., *Dalton. Trans.*, **13**, 2006, p. 1685
35. SUN Y. Q., ZHANG J., YANG G.Y., *Dalton. Trans.*, **18**, 2003, p. 3634
36. DUMITRU R., CARP O., BUDRUGEAC P., NICULESCU M., SEGAL E., *J. Therm. Anal. Calorim.*, **103**, no. 2, 2011, p. 591
37. WEI X., CHEN D., TANG W., *Mat. Chem. Phys.*, **103**, no. 1, 2007, p. 54

Manuscript received: 26.08.2013